bioRxiv preprint doi: https://doi.org/10.1101/2021.11.01.466861; this version posted November 2, 2021. The copyright holder for this preprint (which was not certified by peer review) is the author/funder. All rights reserved. No reuse allowed without permission.

A critical role for E2-p53 interaction during the HPV16 life cycle

Christian T. Fontan[1], Claire D. James[1], Molly L. Bristol[1,4], Apurva T. Prabhakar[1], Raymonde Otoa[1], Xu Wang[1], Elmira Karimi[1], Pavithra Rajagopalan[2], Devraj Basu[2,3] and Iain M. Morgan[1,4*].

[1]Virginia Commonwealth University (VCU), Philips Institute for Oral Health Research, School of Dentistry, Richmond, VA, 23298

[2]Department of Otorhinolaryngology, University of Pennsylvania, Philadelphia, PA 19104

[3]The Wistar Institute Cancer Center, Philadelphia, PA 19104

[4]VCU Massey Cancer Center, Richmond, VA, 23298

*corresponding author, immorgan@vcu.edu

Keywords: human papillomavirus, E2, p53, cervical cancer, head and neck cancer, life cycle, comet assay, senescence, interaction.

bioRxiv preprint doi: https://doi.org/10.1101/2021.11.01.466861; this version posted November 2, 2021. The copyright holder for this preprint (which was not certified by peer review) is the author/funder. All rights reserved. No reuse allowed without permission.

Abstract

Human papillomaviruses (HPV) are causative agents in ano-genital and oral cancers; HPV16 is the most prevalent type detected in human cancers. The HPV16 E6 protein targets p53 for proteasomal degradation to facilitate proliferation of the HPV16 infected cell. However, in HPV16 immortalized cells E6 is predominantly spliced (E6*) and unable to degrade p53. Here we demonstrate that human foreskin keratinocytes immortalized by HPV16 (HFK+HPV16), and HPV16 positive oropharyngeal cancers, retain significant expression of p53. In addition, p53 levels can be increased in HPV16+ head and neck cancer cell lines following treatment with cisplatin. Introduction of full-length E6 into HFK+HPV16 resulted in attenuation of cellular growth (in hTERT immortalized HFK, E6 expression promoted enhanced proliferation). An understudied interaction is that between E2 and p53 and we investigated whether this was important for the viral life cycle. We generated mutant genomes with E2 unable to interact with p53 resulting in profound phenotypes in primary HFK. The mutant induced hyper-proliferation, but an ultimate arrest of cell growth; β-galactosidase staining demonstrated increased senescence, and COMET assays showed increased DNA damage compared with HFK+HPV16 wild type cells. There was failure of the viral life cycle in organotypic rafts with the mutant HFK resulting in premature differentiation and reduced proliferation. The results indicate that the E2-p53 interaction is critical during the HPV16 life cycle, and that disruption of this interaction has anti-viral potential. We discuss potential mechanisms to explain these phenotypes.

bioRxiv preprint doi: https://doi.org/10.1101/2021.11.01.466861; this version posted November 2, 2021. The copyright holder for this preprint (which was not certified by peer review) is the author/funder. All rights reserved. No reuse allowed without permission.

Importance

Human papillomaviruses are causative agents in around 5% of all cancers. There are currently no antivirals available to combat these infections and cancers, therefore it remains a priority to enhance our understanding of the HPV life cycle. Here we demonstrate that an interaction between the viral replication/transcription/segregation factor E2 and the tumor suppressor p53 is critical for the HPV16 life cycle. HPV16 immortalized cells retain significant expression of p53, and the critical role for the E2-p53 interaction demonstrates why this is the case. If the E2-p53 interaction is disrupted then HPV16 immortalized cells fail to proliferate, have enhanced DNA damage and senescence, and there is premature differentiation during the viral life cycle. Results suggest that targeting the E2-p53 interaction would have therapeutic benefits, potentially attenuating the spread of HPV16.

bioRxiv preprint doi: https://doi.org/10.1101/2021.11.01.466861; this version posted November 2, 2021. The copyright holder for this preprint (which was not certified by peer review) is the author/funder. All rights reserved. No reuse allowed without permission.

Introduction:

HPV16 infection causes half of cervical cancers and up to 90% of HPV-positive oropharyngeal cancers (1). Despite advances in vaccination, the prevalence in HPV-associated oropharyngeal cancer continues to rise, contributing to an ongoing public health crisis without any effective anti-viral therapies (2-5).

HPV infects basal epithelial cells and delivers its circular 8kbp DNA genome into the nucleus of the host. Consequently, cellular host factors initiate transcription from the viral long control region (LCR) (6). The viral mRNA is expressed from a single transcript which is then processed, spliced and translated into individual viral proteins. In high-risk HPV infection, the viral oncoproteins E6 and E7 contribute to cellular transformation and cancer progression by targeting several cellular proteins, including tumor suppressors p53 and pRb respectively (7-11).

HPV uses two proteins to initiate replication of the viral episome. The E2 protein homodimerizes via a carboxyl terminus domain and binds to four 12-bp palindromic sequences within the viral LCR and origin (12). Via its amino terminus, E2 recruits the viral helicase E1 to the origin which forms a di-hexamer that replicates the viral genome with the assistance of host polymerases (13, 14). Upon initial infection, the HPV genome replicates to 20-50 copies and maintains this copy number as the infected cell migrates through the epithelium. As the infected cell differentiates and reaches the upper layers, the viral genome amplifies and expresses the L1 and L2 capsid proteins that promote virus assembly and shedding (15-17).

E2 has additional roles in the viral life cycle. E2 can promote or repress viral transcription depending on protein concentration (18). E2 binds to host mitotic chromatin to facilitate viral segregation, resulting in sorting of viral episomes into daughter nuclei following mitosis (19). E2 also regulates expression of host genes important in the viral life cycle and cancer progression (20-24).

bioRxiv preprint doi: https://doi.org/10.1101/2021.11.01.466861; this version posted November 2, 2021. The copyright holder for this preprint (which was not certified by peer review) is the author/funder. All rights reserved. No reuse allowed without permission.

The tumor suppressor p53 primarily functions as a transcription regulatory factor during cellular stress and DNA-damage, leading to cell cycle arrest, senescence, and apoptosis (25-30). In HPV infection, the 150 amino acid E6 oncoprotein interferes with the transcriptional activity of tumor suppressor p53, as well as induces its degradation (7, 9, 31). Direct degradation is initiated by the formation of a complex with p53 and the host partner protein E6AP, which is an ubiquitin ligase. E6 directs the ligase activity of E6AP to p53, promoting its degradation via the proteasome (7, 31-33). This is in direct contrast with many HPV-negative cancers where p53 often becomes mutationally inactivated (34, 35). The degradation of p53 by HPV is also regulated by alternative splicing of high-risk E6 proteins, resulting in a short modulatory isoforms of the oncoprotein such as E6* and E6*I which do not bind to p53 and can inhibit E6-E6AP-p53 complex formation preventing p53 degradation in a cell-cycle specific manner (36-38). We, and others, have reported that expression of alternatively spliced forms of E6 are more dominant compared to full-length E6 in HPV-positive head and neck cancer, and ectopic expression of these isoforms have anti-tumorigenic effects (38-41). The disruption of the E6-E6AP-p53 degradation complex by E6* and E6*I, allowing for p53 expression, suggests that p53 expression may be important in HPV immortalized cells.

Another reported viral interactor with p53 is E2. E2 proteins from high-risk HPVs can bind to p53 and this interaction can trigger apoptosis in cervical cancer cells (42, 43). Additionally, E2 replication function is regulated by this interaction with p53 as overexpression of p53 reduces viral replication (44). This led us to hypothesize that in HPV16 immortalized cells, residual p53 is necessary to maintain a healthy viral life cycle, perhaps via an interaction with E2.

Here, we demonstrate that p53 expression is clearly detectable in a variety of cell lines and tumors immortalized by HPV16 (45, 46). Depletion of residual p53 by overexpression of full length E6 protein led to a significant reduction in cellular proliferation in keratinocytes immortalized by wild-type HPV16. Expression of a mutant E6 protein lacking p53 binding had no effect on cell growth.

bioRxiv preprint doi: https://doi.org/10.1101/2021.11.01.466861; this version posted November 2, 2021. The copyright holder for this preprint (which was not certified by peer review) is the author/funder. All rights reserved. No reuse allowed without permission.

To determine whether an interaction between E2 and p53 was important for cellular proliferation of HPV16 positive cells, we generated an HPV16 genome with point mutations in the E2 gene eliminating p53 binding (42, 43). Keratinocytes were then immortalized by this mutant. Remarkably, compared to wild type HPV16, $E2^{-p53}$ mutant cells, following an initial burst in proliferation, stopped growing and had increased levels of senescence, and accumulated DNA breaks as evidence by single-cell gel electrophoresis assay (COMET). When subjected to differentiation via organotypic raft culturing, these mutant cells had reduced proliferation leading to marked reduction in raft thickness. There was also a reduction in viral replication markers in the mutant cells. These results suggest that although p53 is downregulated by E6 in high-risk HPV infection, p53 is still necessary to permit HPV induced proliferation and that the interaction with E2 plays an important role in the requirement for p53 expression.

Results:

Tumor Suppressor p53 is expressed in HPV16 immortalized cells and is critical for their optimal growth.

Previous studies demonstrated that alternative splice variants (E6*) are the dominant E6 transcripts in HPV associated head and neck cancer, preventing E6-E6AP-p53 complex formation and inhibiting p53 degradation (36-41). We confirmed the presence of p53 in a series of HPV16 positive cell lines (Fig. 1). Expression of the entire HPV16 full genome in N/Tert-1 cells results in partial reduction in p53 compared to near complete abrogation by expression of HPV16 E6 and E7 (Fig. 1A compare lanes 2 and 4 to lane 1). Moreover, human tonsil cells immortalized by HPV16 retain p53 expression near N/Tert-1 control cells (compare lane 1 to 3). To further investigate these findings, we studied two independent donors of human foreskin keratinocytes (HFK) immortalized with HPV16. In both donor lines, p53 levels were much less reduced

bioRxiv preprint doi: https://doi.org/10.1101/2021.11.01.466861; this version posted November 2, 2021. The copyright holder for this preprint (which was not certified by peer review) is the author/funder. All rights reserved. No reuse allowed without permission.

compared to HFK immortalized by HPV16 E6 and E7 overexpression (Lanes 5-8). To determine whether this expression is affected by tumor microenvironment, we surveyed p53 expression in 8 patient derived xenografts (PDX) from oropharyngeal and oral cavity carcinomas (four HPV16 positive and four negative) (45, 46). All HPV16 positive PDX samples and 3 out of 4 HPV negative retained detectable p53 expression illustrating no clear association between HPV status and p53 expression (Fig. 1B**)**. Platinum based DNA-damaging agents such as cisplatin are critical in the treatment of late stage systemic head and neck cancers (47-50). Because DNA-damage is known to stabilize and activate p53, and p53 is most often wild-type in HPV-positive cancers, we predicted that in HPV+ head and neck cancer cell lines the expression of active wild-type p53 can be promoted by cisplatin treatment. We confirmed dose-dependent cisplatin induced p53 expression in SCC-47 and SCC-104 cells (Fig. 1C). These results indicate that p53 expression is conserved in many cell lines immortalized by the HPV16 genome and can be induced by treatment with DNA-damage. This suggests that although E6 degrades p53 to help promote cell immortalization and carcinogenesis, p53 often retains expression under a variety of conditions, indicating that it still may play an important role in the HPV16 life-cycle.

To determine whether reduction of p53 would compromise the growth of HPV16 immortalized cells we introduced full length E6 (using a retroviral delivery of the E6 gene which does not allow alternative splicing) into N/Tert-1 (foreskin keratinocytes immortalized by telomerase) and HFK+HPV16 cells. Fig. 2A demonstrates that the additional expression of E6 in N/Tert-1 cells results in significantly increased cellular proliferation as has been described (51). However, introduction of E6 into HFK+HPV16 resulted in an attenuation of cell growth (Fig. 2B). Because E6 possesses a variety of mechanisms for regulating cellular proliferation independent from p53 degradation, we attempted to isolate these other mechanisms by expressing an E6 mutant unable to promote degradation of p53 but retains all other known functions (52). This mutant did not have a deleterious effect on cell growth indicating that it is the E6 targeting of p53 that results in the

bioRxiv preprint doi: https://doi.org/10.1101/2021.11.01.466861; this version posted November 2, 2021. The copyright holder for this preprint (which was not certified by peer review) is the author/funder. All rights reserved. No reuse allowed without permission.

158 attenuation of cellular proliferation. Additionally, we found that these proliferation rates were
159 inversely correlated with senescence levels (Fig. 2C and 2D). In the HFK+HPV16+E6 cells, we
160 noticed that over time the cells began proliferating once again. To determine whether the
161 recovered cells had a restoration of p53 protein levels we carried out western blots of
162 HFK+HPV16+E6 cells at different stages following E6 introduction (Fig. 2E). Lane 4 demonstrates
163 that there is an initial reduction in p53 protein levels in these cells immediately following selection
164 compared with control cells (compare lane 4 with lane 3). However, following 13 days of culturing
165 (when we noticed proliferation begin to restore to that of the control cells) there is a restoration of
166 p53 protein expression (compare lane 7 with lane 4). These results suggest that reduction of p53
167 protein may lead to growth attenuation and enhanced senescence of HFK+HPV16 cells. They
168 also suggest that to begin to proliferate again, restoration of p53 likely helps promote growth in
169 the HFK+HPV16+E6 cells. We monitored the exogenous E6 RNA levels (Fig 2F). There is a clear
170 reduction in the E6 RNA expressed from the exogenous vector between days 0 and 13 correlating
171 with the restoration of p53 protein expression and cellular proliferation. When we analyzed for E6
172 protein expression via western blot, while we did not notice an appreciable change in E6 protein
173 levels, we found that there was a significant increase of E6Δp53 expression compared to wild-
174 type E6 at both time points (Fig. 2G). This supports our claim that expression of E6 is more
175 deleterious to growth than E6Δp53 in HFK+HPV16 and this is most likely due to p53 degradation.

176 Overall, these results demonstrate that p53 is expressed in HPV16 immortalized cells, and that
177 this expression may be critical for continuing proliferation of these cells. We next moved on to
178 investigate possible reasons for the requirement of p53 expression in HFK+HPV16 cells.

179 **Disruption of p53 interaction with the HPV16 E2 protein attenuates cell growth and blocks**
180 **the viral life cycle**

181 A known and relatively understudied interaction of p53 with HPV16 is the direct physical
182 interaction with E2 (43). We generated an E2 mutant predicted to not interact with p53 ($E2^{-p53}$)

bioRxiv preprint doi: https://doi.org/10.1101/2021.11.01.466861; this version posted November 2, 2021. The copyright holder for this preprint (which was not certified by peer review) is the author/funder. All rights reserved. No reuse allowed without permission.

and generated stable N/Tert-1 cell lines expressing this mutant, as we have done for wild type E2 (43). There was robust, stable expression of E2 and E2^{-p53} in N/Tert-1 cells (Fig. 3A, lane 3). Immunoprecipitation with a p53 antibody brought down p53, and E2 wild type co-immunoprecipitated with p53 while E2^{-p53} did not (Fig. 3B, compare lanes 2 and 3). To demonstrate that E2^{-p53} was functional we carried out transcriptional studies in N/Tert-1 cells. Because the binding of p53 takes place in the DNA-binding domain (DBD) of E2, we confirmed that the mutant E2 retained DNA-binding function. Both E2 wild type and E2^{-p53} were able to repress transcription from the HPV16 long control region (LCR) efficiently and comparatively (Fig. 3C). We also measured that transcriptional activation function of E2 wild type and E2^{-p53} (Fig. 3D). While E2^{-p53} is able to activate transcription it was compromised when compared with E2 wild type (compare lanes 5-7 with lanes 2-4). We conclude from these experiments that E2^{-p53} is nuclear and able to bind to its DNA target sequences but that its transcriptional activation property (but not repression) is attenuated.

Having confirmed that the E2^{-p53} mutant was functional, we introduced the mutations that abrogate the E2-p53 interaction into the entire HPV16 genome (HPV16^{-p53}). We introduced the wild type and mutant HPV16 genomes into 2 independent primary human foreskin cell populations that we recently used to investigate the role of the E2-TopBP1 interaction in the viral life cycle (53). Both the wild type and mutant genomes efficiently immortalized both HFK donor cells. We carried out Southern blotting on *SphI* cut DNA (a single cutter for the HPV16 genome) (Fig. S1A). To further characterize the status of the genomes in these cells we used TV exonuclease assays (this assay is based on the fact that episomal HPV16 genomes are resistant to exonuclease digestion) (54, 55). This assay demonstrated that the viral DNA in the immortalized donor cell lines retained a predominantly episomal status, irrespective of whether the viral genomes were wild type or HPV16^{-p53} (Fig. S1B).

bioRxiv preprint doi: https://doi.org/10.1101/2021.11.01.466861; this version posted November 2, 2021. The copyright holder for this preprint (which was not certified by peer review) is the author/funder. All rights reserved. No reuse allowed without permission.

Next, we investigated the expression of markers relevant to HPV infection in HFKs. Fig. 4A demonstrates that p53 levels are similarly reduced in HFK+HPV16 and HFK+HPV16^{-p53} cells when compared with N/Tert-1 cells (compare lanes 2-5 with lane 1) (Fig. 4B). For comparison, cells immortalized with an E6/E7 expression vector had almost no p53 expression (lane 6), likely due to the inability of the E6 to be spliced to E6* variants with this expression vector. To further characterize these cell lines, we investigated whether the DNA damage response is turned on as HPV infections activate both the ATR and ATM pathways. We investigated the phosphorylation status of CHK1 and CHK2 as surrogate markers for activation of these DNA damage response kinases (Fig. 4D). Compared with N/Tert-1 cells there is an overall increase of CHK1 and CHK2 levels in cells immortalized with HFK+HPV16, HFK+HPV16^{-p53} or E6/E7 expression. CHK1 and CHK2 phosphorylation is also elevated in the presence of all of the HPV16 positive cells when compared with N/Tert-1 cells. It is important to note that E6 and E7 immortalization of HFK induced phosphorylation of CHK1 but not CHK2 when compared with the entire genome (Lane 6). This is likely due to the ATM pathway being largely activated by viral replication rather than by the viral oncogenes E6 and E7 which we have previously reported (56). Overall, these results suggest that markers of HPV16 infection are activated in HFK cells immortalized with HPV16 irrespective of the ability of p53 to bind E2.

Even though the HFK+HPV16^{-p53} cells had markers indicative of HPV16 immortalization, we noticed an aberrant growth phenotype in both foreskin donor cells (Fig. 5A). There was an initial enhanced proliferation of the HFK+HPV16^{-p53} cells when compared with HFK+HPV16. However, around the 3-4 week mark, the HFK+HPV16^{-p53} cells began to slow their growth and eventually stopped proliferating. To determine the mechanism of the attenuation of cell growth we investigated senescence in N/Tert-1, HFK+HPV16 and HFK+HPV16^{-p53} cells by staining for beta-galactosidase (Fig. 5B). There was a significantly increased number of senescent cells with the p53 mutant cells and this was quantitated (Fig. 5C). Senescence can be induced by increased

bioRxiv preprint doi: https://doi.org/10.1101/2021.11.01.466861; this version posted November 2, 2021. The copyright holder for this preprint (which was not certified by peer review) is the author/funder. All rights reserved. No reuse allowed without permission.

DNA damage, particularly double strand breaks (DSB) (25, 26). Because CHK1 and CHK2 pathway activation was not noticeably different between HFK+HPV16 and HFK+HPV16^{-p53}, we decided to look at DSBs more directly using single-cell gel electrophoresis (COMET assay). As expected, the expression of wild type or mutant HPV16 genomes in HFKs led to increased formation of DSBs as indicated by olive tail moment (OTM) when compared to HPV negative N/Tert-1 cells (57) (Fig. 6D). However, the mutant HFKs consistently exhibited larger OTM values compared to HFK+HPV16 (Fig. 5D and 5E). As the expression of full-length E6 from a heterologous vector attenuates the growth of HFK+HPV16 wild type cells (Fig. 2) we rationalized that expression of E6 should not alter the growth of HFK+HPV16^{-p53} cells. Stable expression of exogenous full length E6 or the E6Δp53 mutant had no additional effect on the proliferation of HFK+HPV16^{-p53} cells, illustrating that the drastic differences in proliferation are potentially due to the E2-p53 interaction (Fig. 5F).

HFK+HPV16^{-p53} cells have an aberrant life cycle in differentiating epithelium.

We organotypically rafted HFK+HPV16 and HFK+HPV16^{-p53}. Both lines were placed on collagen plugs at early passage when the HFK+HPV16^{-p53} cells retained proliferative capacity. Due to the large difference in growth rates between the wild type and mutant cells, the original plating was performed with both 1x10^6 and 2x10^6 cells to promote production of a monolayer on the collagen plugs prior to lifting to the liquid-air interface for differentiation. Fig 6A demonstrates an aberrant differentiation process with the HFK+HPV16^{-p53} cells when compared with HFK+HPV16 cells at both cell densities. It is noticeable that at the lower cell density (1x10^6) there was a failure to form a monolayer prior to induction of differentiation (as evidenced by gaps between keratinocyte cell clusters on the collagen plug). Using a seeding density of 2x10^6 eliminated the formation of gaps but did not improve the proliferation. A representative of two independent donors is shown, both donors had identical phenotypes. Fig. 6B quantitates the results from two independent rafts from two independent donors; the mutant genomes have dramatically lower raft area when compared

bioRxiv preprint doi: https://doi.org/10.1101/2021.11.01.466861; this version posted November 2, 2021. The copyright holder for this preprint (which was not certified by peer review) is the author/funder. All rights reserved. No reuse allowed without permission.

with wild-type genomes. To investigate whether differentiation has occurred in these cells we stained with Involucrin and Keratin 10 (Fig. 6C). The mutant genome cells stained positive for both differentiation markers demonstrating that, even though raft growth is markedly attenuated, differentiation still occurs. We also stained for viral replication using the DNA-damage marker γ-H2AX. Recently we reported that an E2 mutant that failed to interact with TopBP1 results in degradation of E2 during organotypic rafting; this degradation would block viral replication and indeed these cells had no γ-H2AX staining (53). This demonstrates that the γ-H2AX staining indicates the occurrence of viral replication. Fig. 6D demonstrates that there is abundant nuclear γ-H2AX staining throughout HFK+HPV16 cells, indicating replication is occurring. The HFK+HPV16^{-p53} cells also support viral replication although there is a reduction in the number of rafted cells stain positively for γ-H2AX (Fig. 6D).

Discussion:

The HPV E2 protein is essential for viral genome replication, segregation of viral episomes into daughter cells following cell division, and can transcriptionally regulate both virus and host genomes (12, 19, 20). E2 interacts with a variety of host factors to promote progression of the viral life cycle, many of which are essential such as interactions with TopBP1 and BRD4 (12, 19, 23, 53, 58). In this report, we propose that E2 binding to p53 is also an essential interaction as abrogation of the interaction leads to catastrophic failure of the viral life cycle.

In the classical high-risk HPV model, upon initial infection, the viral oncogenes E6 and E7 inhibit and degrade tumor suppressor proteins p53 and pRb respectively, promoting hyperproliferation, unregulated DNA replication, mutation accumulation and potentially eventual carcinogenesis. Therefore, immortalization of cell lines can be achieved with overexpression vectors of E6 and E7 (Fig. 1A, Lanes 4 and 8). Previous studies suggest that E6 splice variants and their action on E6-E6AP-p53 complex disruption is cell-cycle dependent (38). In HPV18 cell lines, E6*I shows marked upregulation during and p53 restoration during G2/M (38). We have previously illustrated

bioRxiv preprint doi: https://doi.org/10.1101/2021.11.01.466861; this version posted November 2, 2021. The copyright holder for this preprint (which was not certified by peer review) is the author/funder. All rights reserved. No reuse allowed without permission.

that E2 is stabilized during mitosis which is important for its association with TopBP1 and its role as a segregation factor (53). It is entirely possible that the cell-cycle mediated p53 restoration corresponds with E2 stabilization allowing these proteins to interact, and may also play an important role in genome segregation.

E2 can regulate host transcription in a multitude of ways. We recently reported that E2 can epigenetically repress the TWIST1 at the histone level, inhibiting EMT and promoting a less aggressive cellular phenotype (20). E2 can also promote the recruitment of DNA methyltransferase 1 to interferon response genes, resulting in DNA base methylation and global innate immunity downregulation (21). It is currently unclear how E2 recruits epigenetic modifiers to these genes and p53 may play an important role. DNA methyltransferases (DMNTs) are often part of large multimeric complexes and use transcription regulatory proteins to help target specific genes undergoing epigenetic silencing (59, 60). p53 is known to also interact with DMNT1 resulting in the methylation of antiapoptotic genes (61). It is possible that the interaction between E2 and p53 is important for the rerouting of DNMTs to different genes whose regulation is important for a healthy viral life cycle. It is also noticeable that E2-p53 has an attenuated ability to activate transcription (Fig. 3), indicating that regulation of host gene transcription by E2 may require co-operation with p53 in some cases.

The results from Fig. 5D suggest that additional double strand breaks play a role in the enhanced damage and proliferation rate of HFK+HPV16-p53 mutant cells compared to wild type immortalized HFKs. HPV uses homologous recombination (HR) factors to assist in viral replication (62-64). Conversely, p53 binds to replication protein A (rpA) resulting in repression of HR, reducing DSB repair and promoting apoptosis during catastrophic genome instability (27, 29). It is possible that E2 helps regulate this activity of p53 and inability to do so results in accumulation of DSBs as seen in Fig. 5D.

bioRxiv preprint doi: https://doi.org/10.1101/2021.11.01.466861; this version posted November 2, 2021. The copyright holder for this preprint (which was not certified by peer review) is the author/funder. All rights reserved. No reuse allowed without permission.

306 In conclusion, this report indicates that p53 expression is retained in HPV16 positive cell lines and
307 tumor samples under a variety of conditions. Depletion of this residual p53 by full length E6 results
308 in significant reduction in proliferation and enhanced senescence in cells immortalized with
309 HPV16 which we attribute to loss of E2 interaction with p53. Human foreskin cells immortalized
310 by HPV16 where E2 can no longer bind to p53 exhibit aberrant phenotypes including dysregulated
311 proliferation, enhanced levels of DSBs and overall failure of the viral life cycle during organotypic
312 raft culturing. Due to the importance of p53 in the context of HPV related cancers as well as the
313 profound phenotypes demonstrated in this report, further investigation on the interaction between
314 E2 and p53 is warranted.

315

316 **Methods:**

317 **Cell culture.** N/Tert-1 cells and head-and-neck cancer lines UMSCC47 and UMSCC104 were
318 cultured as previously described (20, 21, 65-67). Immortalization and culturing of human foreskin
319 keratinocytes with HPV16 are described below. Cells were incubated at 37°C and 5% CO2 with
320 media changed every 3 days. For cisplatin treatment, cells were incubated with indicated
321 concentrations of drug dissolved in DMF or DMF vehicle control for 24-hours

322 **Immortalization of human foreskin keratinocytes (HFK).** HPV16 mutant genome (HPV16-p53,
323 which contained an E2 unable to bind p53) was generated and sequenced by Genscript (42, 44,
324 68). Residues Aspartic acid 388, Tryptophan 341 and Aspartic acid 344 were all mutated to
325 alanine resulting in inability for E2 to interact with p53. The HPV16 genome was removed from
326 the parental plasmid using *SphI*, and the viral genomes isolated and then re-circularized using T4
327 ligase (NEB) and transfected into early passage HFK from three donor backgrounds (Lifeline
328 technology), alongside a G418 resistance plasmid, pcDNA. Cells underwent selection in 200
329 μg/mL G418 (Sigma-Aldrich) for 14 days and were cultured on a layer of J2 3T3 fibroblast feeders

bioRxiv preprint doi: https://doi.org/10.1101/2021.11.01.466861; this version posted November 2, 2021. The copyright holder for this preprint (which was not certified by peer review) is the author/funder. All rights reserved. No reuse allowed without permission.

(NIH), which had been pre-treated with 8 µg/ml mitomycin C (Roche). Throughout the immortalization process, HFK were cultured in Dermalife-K complete media (Lifeline Technology).

Western blotting. Protein from cell pellets was extracted with 2x pellet volume protein lysis buffer (0.5% Nonidet P-40, 50mM Tris [pH 7.8], and 150mM NaCl) supplemented with protease inhibitor (Roche Molecular Biochemicals) and phosphatase inhibitor cocktail (Sigma). Protein extraction from patient derived xenografts was performed as previously described.(45, 46) The cells were lysed on ice for 30 min followed by centrifugation at 18,000 rcf (relative centrifugal force) for 20 min at 4°C. Protein concentration was estimated colorimetrically using a Bio-Rad protein assay and 25 µg of protein with equal volume of 2X Laemmli sample buffer (Bio-Rad) was denatured at 70ºC for 10 min. The samples were run on a Novex™ WedgeWell™ 4 to 12% Tris-glycine gel (Invitrogen) and transferred onto a nitrocellulose membrane (Bio-Rad) using the wet-blot method, at 30 V overnight. The membrane was blocked with *Li-Cor* Odyssey® blocking buffer (PBS) diluted 1:1 v/v with PBS for 1 hour at room temperature and then incubated with specified primary antibody in *Li-Cor* Odyssey® blocking buffer (PBS) diluted 1:1 with PBS. Afterwards, the membrane was washed with PBS supplemented with 0.1% Tween20 and further probed with the Odyssey secondary antibodies (IRDye® 680RD Goat anti-Rabbit IgG (H + L), 0.1 mg or IRDye® 800CW Goat anti-Mouse IgG (H + L), 0.1 mg) in *Li-Cor* Odyssey® blocking buffer (PBS) diluted 1:1 with PBS at 1:10,000 for 1 hour at room temperature where applicable. After washing with PBS-tween, the membrane was imaged using the Odyssey® CLx Imaging System and ImageJ was used for quantification. Primary antibodies used for western blotting studies are as follows: p53, 1:1000 (Santa Cruz; cat. no. sc-47698) HPV16 E2, 1:1000 (TVG261) (Abcam; cat. no. ab17185) phospho-CHK1, 1:1000 (Ser345) (Cell Signaling; cat. No. 2341S), phosphor CHK2 (Thr68), 1:1000 (Cell Signaling; cat. No. 2661S), CHK1, 1:1000(Cell Signaling; cat. No. 2360), CHK2, 1:1000 (Abcam; cat. No. ab47443), GAPDH, 1:250 (Santa Cruz; cat. no. sc-47724).

bioRxiv preprint doi: https://doi.org/10.1101/2021.11.01.466861; this version posted November 2, 2021. The copyright holder for this preprint (which was not certified by peer review) is the author/funder. All rights reserved. No reuse allowed without permission.

Plasmids. The following plasmids were used the completion of these studies: pMSCV-N-FLAG-HA-GFP, pMSCV-N-FLAG-HA-HPV16E6, pMSCV-IP-N-FLAG-HA-16E6 8S9A10T ("E6Δp53"). Wild-type 16E2 or 16E2-p53 (Mutated residues W341A, D344A, D338A) were cloned into pCDNA vector for confirmation of p53 interaction in N/Tert-1 cells. pCDNA was used for empty vector control.

Real-time qPCR. RNA was isolated using the SV Total RNA isolation system (Promega) according to manufacturer's instructions. 2 µg of RNA was reverse transcribed into cDNA using the high-capacity reverse transcription kit (Applied Biosystems). The PowerUp SYBR green master mix (Applied Biosystems) was used along with cDNA and gene specific primers and real-time PCR was performed using a 7500 Fast real-time PCR system as previously described. (20, 21, 65) Expression was quantified as relative quantity over GAPDH using the $2^{-\Delta\Delta C_T}$ method. Primers used are as follows. FLAG-HA Tag fwd 5'- GACTACAAGGATGACGATG- 3', FLAG-HA Tag rev 5'- GCGTAATCTGGAACATCG -3'.

p53 Immunoprecipitation. Primary polyclonal antibody against p53 (Invitrogen; PA5-27822) or a HA-tag antibody (used as a negative control) was incubated in 200 µg of cell lysate (prepared as described above), made up to a total volume of 500 µl with lysis buffer (0.5% Nonidet P-40, 50mM Tris [pH 7.8], and 150mM NaCl), supplemented with protease inhibitor (Roche Molecular Biochemicals) and phosphatase inhibitor cocktail (Sigma) and rotated at 4°C overnight. The following day, 50 µl of pre-washed protein A-sepharose beads per sample was added to the lysate/antibody solution and rotated for 4 hours at 4°C. The samples were gently washed with 500 µl lysis buffer by centrifugation at 1,000 rcf for 2-3 min. This wash was repeated 4 times. The bead pellet was resuspended in 4X Laemmli sample buffer (Bio-Rad), heat denatured and centrifuged at 1,000 rcf for 2-3 min. Proteins were separated using an SDS-PAGE system and transferred onto a nitrocellulose membrane before probing for the presence of E2 or p53, as per western blotting protocol.

bioRxiv preprint doi: https://doi.org/10.1101/2021.11.01.466861; this version posted November 2, 2021. The copyright holder for this preprint (which was not certified by peer review) is the author/funder. All rights reserved. No reuse allowed without permission.

Transcription and LCR Repression assays. A pTK6E2-Luciferace reporter plasmid was utilized to analyze transcriptional activation of Wild-type HPV16 E2 and E2Δp53 proteins as previously described (23). $5x10^5$ N/Tert-1 cells were seeded onto $100mm^2$ plate and transfected 24 hours later with 0 ng, 10 ng, 100 ng or 1000 ng of E2 WT or $E2^{-p53}$ plasmid DNA along with 1000ng of pTK6E2-Luciferase reporter plasmid using Lipofectamine 2000 according to the manufacturer's instructions (ThermoFisher Scientific). Cells were harvested the next day using Promega luciferase assay system. For LCR repression activity, a pHPV16-LCR-Luciferase reporter was used in place of the pTK6E2-Luciferase plasmid.(65)

Southern blotting. Total cellular DNA was extracted by proteinase K-sodium dodecyl sulfate digestion followed by a phenol-chloroform extraction method. 5 µg of total cellular DNA was digested with either SphI (to linearize the HPV16 genome) or HindIII (which fails to cut HPV16 genome). All digestions included DpnI to ensure that all input DNA was digested. All restriction enzymes were purchased from NEB and utilized as per manufacturer's instructions. Digested DNA was separated by electrophoresis of a 0.8% agarose gel, transferred to a nitrocellulose membrane, and probed with radiolabeled (32-P) HPV16 genome as previously described.(67) This was then visualized by exposure to film for 1 to 24 hours. Images were captured from an overnight-exposed phosphor screen by GE Typhoon 9410 and quantified using ImageJ.

Exonuclease V assay. PCR based analysis of viral genome status was performed using methods described by Myers et al (2019). Briefly, 20 ng genomic DNA was either treated with exonuclease V (RecBCD, NEB), in a total volume of 30 µl, or left untreated for 1 hour at 37°C followed by heat inactivation at 95°C for 10 minutes. 2 ng of digested/undigested DNA was then quantified by real time PCR using a 7500 FAST Applied Biosystems thermocycler with SYBR Green PCR Master Mix (Applied Biosystems) and 100 nM of primer in a 20 µl reaction. Nuclease free water was used in place of the template for a negative control. The following cycling conditions were used: 50°C for 2 minutes, 95°C for 10 minutes, 40 cycles at 95°C for 15 seconds, and a dissociation stage of

bioRxiv preprint doi: https://doi.org/10.1101/2021.11.01.466861; this version posted November 2, 2021. The copyright holder for this preprint (which was not certified by peer review) is the author/funder. All rights reserved. No reuse allowed without permission.

95°C for 15 seconds, 60°C for 1 minute, 95°C for 15 seconds, and 60°C for 15 seconds. Separate PCR reactions were performed to amplify HPV16 E6 F: 5'- TTGCTTTTCGGGATTTATGC-3' R: 5'- CAGGACACAGTGGCTTTTGA-3', HPV16 E2 F: 5'- TGGAAGTGCAGTTTGATGGA-3' R: 5'-CCGCATGAACTTCCCATACT-3', human mitochondrial DNA F: 5'-CAGGAGTAGGAGAGAGGGAGGTAAG-3' R: 5'-TACCCATCATAATCGGAGGCTTTGG -3', and human GAPDH DNA F: 5'- GGAGCGAGATCCCTCCAAAAT-3' R: 5'-GGCTGTTGTCATACTTCTCATGG-3'

Senescence Staining. $7.5x10^4$ cells were seeded in 6-well plates. The following day, cells were stained for senescence using the Cell Signal Senescence β-Galactosidase Staining kit according to manufacturer's instructions (9860). Randomly selected images were taken using the Keyence imaging system at 10X. Positively stained cells were counted by a blinded observer and average number of positively stained cells per field were calculated.

Single-cell gel electrophoresis (COMET) Assay. $1x10^4$ cells were plated in 24-well plate with 1mL media one day prior to harvest. The next day, cells were trypsinized and resuspended in a mixture 0.5% w/v Low molecular weight agarose (Lonza, cat. No. #50101) and PBS at a ratio of 10:1. Suspension was immediately pipetted onto Trivegen COMET Slides™ (4250-004-03) and allowed to dry for 30 min at 4°C. Slides underwent lysis for 90 min at 4°C in the dark (Lysis buffer: 10mM Tris, 100mM EDTA, 2.5M NaCl, 1% TritonX100, 10%DMSO titrated to pH 10.0). Afterwards slides were placed in Alkaline buffer for 25 min at at 4°C in the dark (Alkaline buffer: 1mM EDTA, 200mM NaOH, pH >13.0). Slides were transferred to an agarose gel electrophoresis box filled with additional alkaline buffer. Electrophoresis was performed at 25V for 20min at room temperature in the dark. Slides were then washed 2x in dd (double distilled) H2O for 5 min at RT and then placed in neutralization buffer for 20min at RT in dark (Neutralization buffer: 400mM Tris-HCl titrated to pH 7.5). Neutralized slides were then left to dry at 37°C in the dark. Dried slides were stained with DAPI (1:10,000 in dd H2O) for 15 min at RT then washed 2x with dd H20 for 5 min. Stained and rinsed slides were left to dry overnight. Slides were imaged using the

bioRxiv preprint doi: https://doi.org/10.1101/2021.11.01.466861; this version posted November 2, 2021. The copyright holder for this preprint (which was not certified by peer review) is the author/funder. All rights reserved. No reuse allowed without permission.

Keyence imaging system at 20x with >5 images taken per replicate. Quantization of olive tail moments (OTM) was achieved using the CASPLab COMET Assay imaging software by Końca K et al, 2003 (69).

Organotypic raft culture. Keratinocytes were differentiated via organotypic raft culture as described previously.(21, 67, 70) Briefly, cells were seeded onto type 1 collagen matrices containing J2 3T3 fibroblast feeder cells. Cells were cultured to confluency atop the collagen plugs, lifted onto wire grids and cultured in cell culture dishes at the air-liquid interface. Media was replaced on alternating days. Following 14 days of culture, rafted samples were fixed with formaldehyde (4% v/v) and embedded in paraffin. Multiple 4μm sections were cut from each sample. Sections were stained with hematoxylin and eosin (H&E) and others prepared for immunofluorescent staining via HIER. Fixing and embedding services in support of the research project were generated by the VCU Massey Cancer Center Cancer Mouse Model Shared Resource, supported, in part, with funding from NIH-NCI Cancer Center Support Grant P30 CA016059. Fixed sections were antigen retrieved in citrate buffer, and probed with the following antibodies for immunofluorescent anaylsis: phospho-yH2AX 1/500 (Cell Signaling Technology; 9718), Involucrin 1/1000 (abcam; ab27495), Keratin 10 1/1000 (SigmaAldrich; SAB4501656), and HPV16 E2. (monoclonal B9)(71) Cellular DNA was stained with 4’,6-diamidino-2-phenylindole (DAPI, Santa Cruz sc-3598). Microscopy was performed using the Keyence imaging system,

bioRxiv preprint doi: https://doi.org/10.1101/2021.11.01.466861; this version posted November 2, 2021. The copyright holder for this preprint (which was not certified by peer review) is the author/funder. All rights reserved. No reuse allowed without permission.

Acknowledgements:

This work was supported by VCU Philips Institute for Oral Health Research and the National Cancer Institute designated Massey Cancer Center grant P30 CA016059 (IMM). DB is supported by R01DE027185, a grant from the National Institute of Dental and Craniofacial Research.

bioRxiv preprint doi: https://doi.org/10.1101/2021.11.01.466861; this version posted November 2, 2021. The copyright holder for this preprint (which was not certified by peer review) is the author/funder. All rights reserved. No reuse allowed without permission.

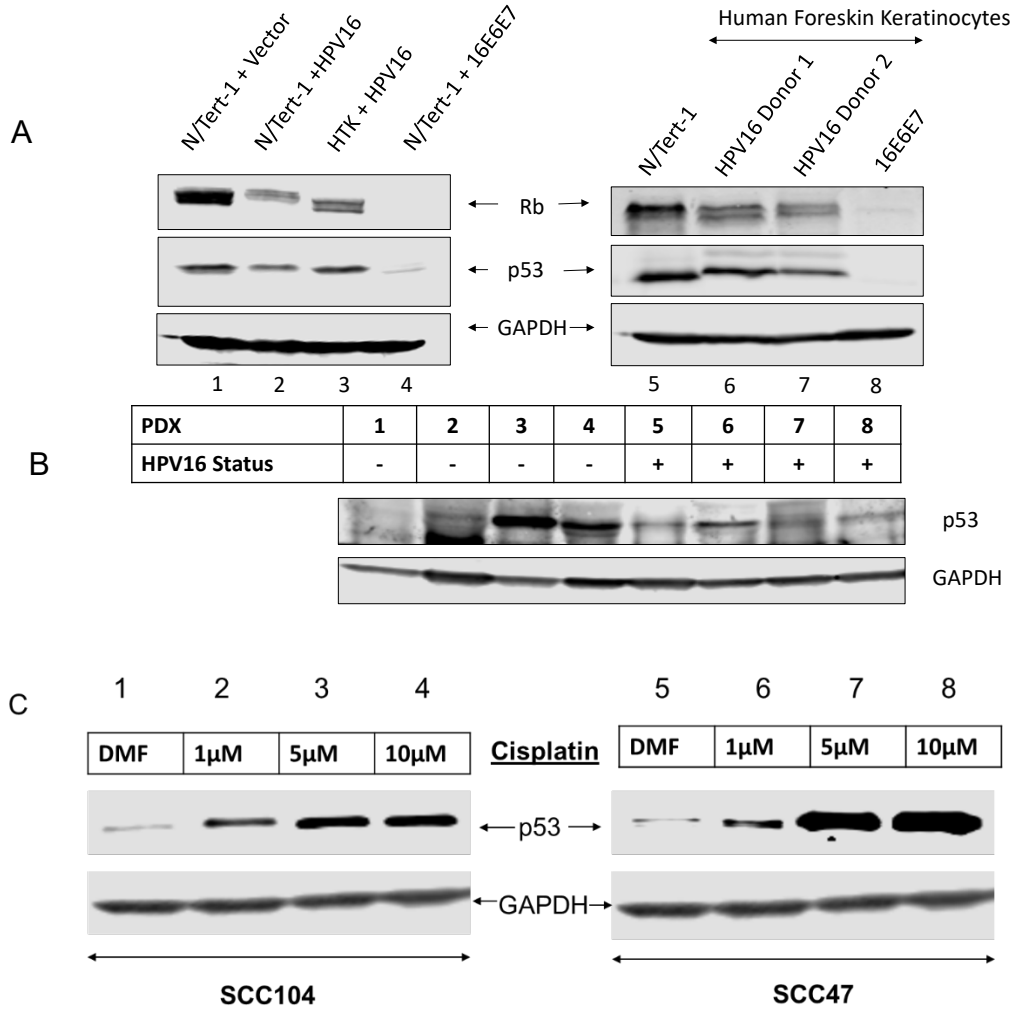

464 **Figure 1. Tumor suppressor p53 expression is conserved in HPV16 immortalized cell lines**
465 **and patient derived xenografts** (A) Western blot analysis of p53 and pRb in N/tert-1 cells stably
466 expressing the HPV16 genome (lane 2), HPV16 E6+E7 (lane 4) or empty vector (lane 1)
467 compared to Human tonsillar keratinocytes immortalized with HPV16 (lane 3). Two independent
468 human foreskin keratinocyte (HFK) donors were immortalized with wild-type HPV16 (lanes 6 and
469 7) or overexpression of HPV16 E6 and E7 oncogenes (lane 8, cells from donor 1). (B) Western
470 blot analysis of p53 expression in 4 HPV-negative and 4 HPV-positive patient derived xenografts.
471 (C). p53 expression following 24-hour cisplatin treatment of primary HPV-positive head and neck

bioRxiv preprint doi: https://doi.org/10.1101/2021.11.01.466861; this version posted November 2, 2021. The copyright holder for this preprint (which was not certified by peer review) is the author/funder. All rights reserved. No reuse allowed without permission.

472 cancer cell lines (SCC47 and SCC104) DMF solvent only was used as drug-free control. All

473 western blots utilized GAPDH as an internal loading control.

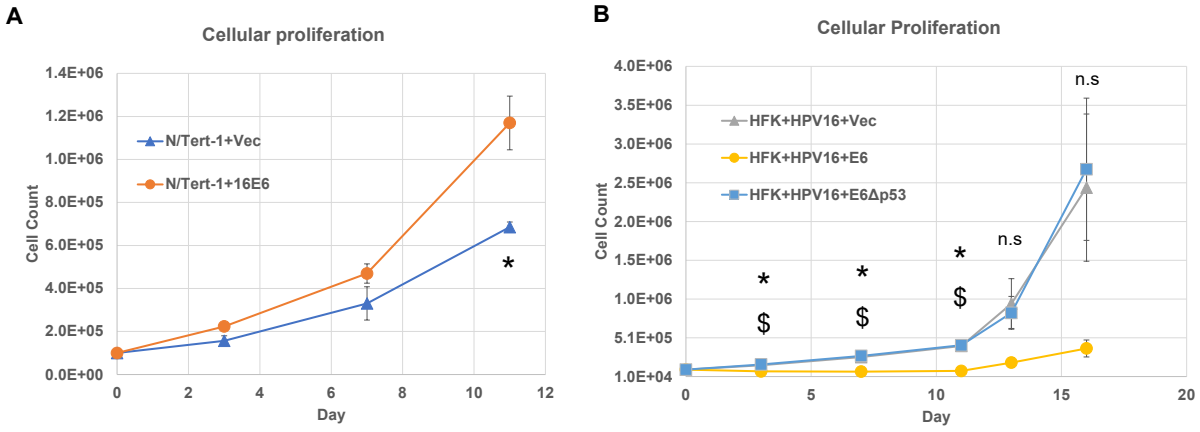

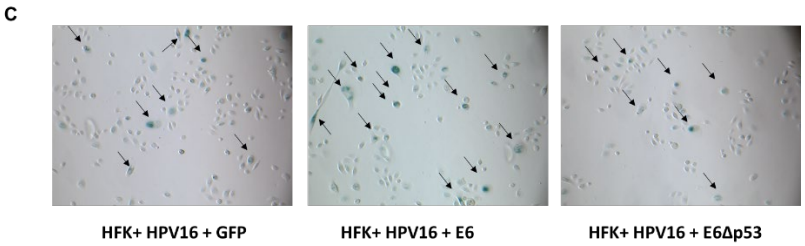

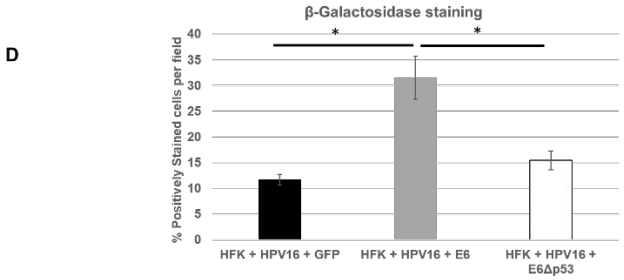

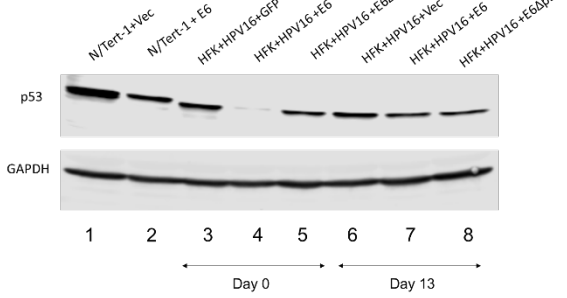

475

476

477

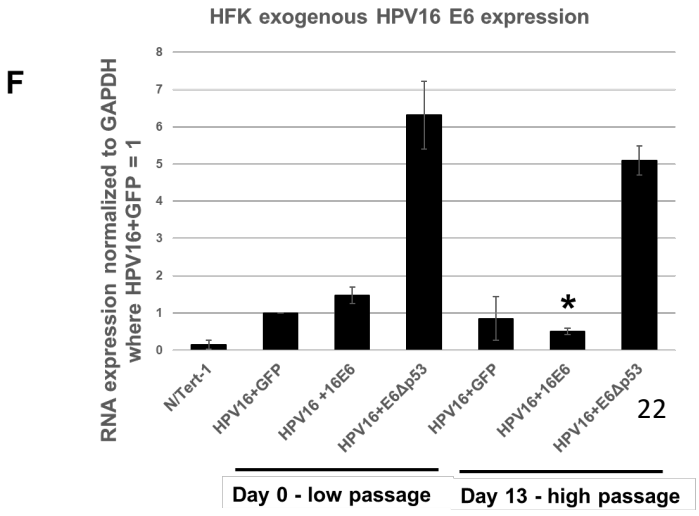

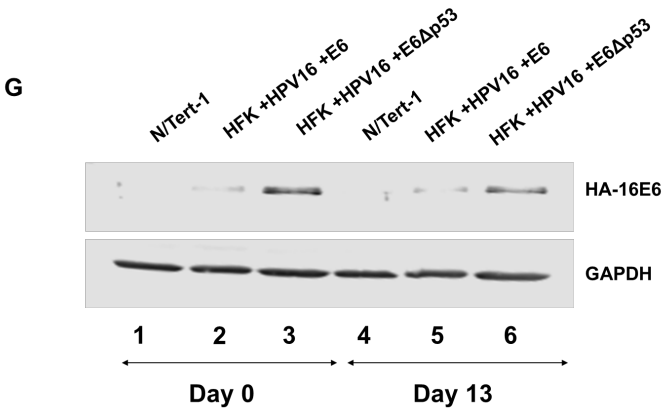

bioRxiv preprint doi: https://doi.org/10.1101/2021.11.01.466861; this version posted November 2, 2021. The copyright holder for this preprint (which was not certified by peer review) is the author/funder. All rights reserved. No reuse allowed without permission.

Figure 2. p53 reduction in via introduction of full length HPV16 E6 reduces cellular proliferation in HPV16 immortalized foreskin keratinocytes. (A) 11-day growth curve of N/Tert-1 cells expressing exogenous HPV16 E6 compared to empty vector. (B) 13-day growth curve of human foreskin keratinocytes immortalized by HPV16 and stably expressing exogenous full length E6, mutant E6 that does not bind and degrade p53 (E6Δp53) or GFP control vector. (C) Senescence staining of cells in B at day 11. Arrows indicate positively staining cells. (D) Quantification of senescence staining in C. Western blot analysis of p53 expression following transfection of E6 plasmids (day 0) and after growth rate recovery of HFK+HPV16+E6 (day 13). (E) Western blot analysis of exogenous E6 and E6Δp53 expression at day 0 and day 13 using primary antibody against HA tag. HFK+GFP samples were omitted due to signal oversaturation and bleed over into neighboring wells. GAPDH was used as internal loading control. (F) RT-qPCR analysis of exogenous GFP, E6 and E6Δp53 expression at day 0 and day 13 using primers against FLAG-HA tag. Relative quantity calculated by the $\Delta\Delta C_T$ method using GAPDH as an internal control. Bonferroni correction utilized when applicable. (G) Western blotting of the indicated extracts using FLAG antibody (the E6 is double tagged with HA and FLAG).

bioRxiv preprint doi: https://doi.org/10.1101/2021.11.01.466861; this version posted November 2, 2021. The copyright holder for this preprint (which was not certified by peer review) is the author/funder. All rights reserved. No reuse allowed without permission.

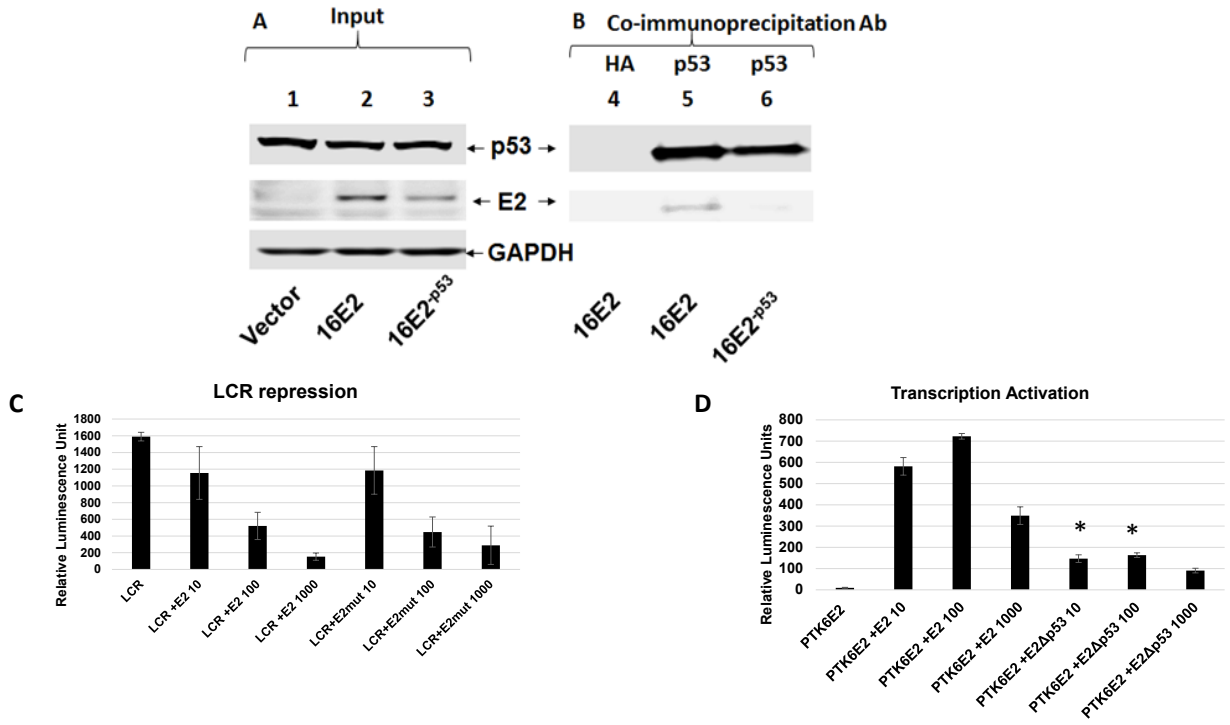

Figure 3. Generation and characterization of p53 binding mutant of HPV16 E2 (E2-p53) in N/Tert-1 cells. (A) Input western blot of stably expressing E2 and E2^{-p53} in N/Tert-1 Cells. For E2^{-p53}, residues W341, D344 and D338 were mutated to alanine as previously described (42, 43). (B) Co-immunoprecipitation pull down of E2 using polyclonal antibody against p53. (C) HPV16 long control region repression assay of wild-type E2 and E2^{-p53}. N/Tert-1 cells were transiently transfected with 1 µg pHPV16-LCR-Luciferase reporter plasmid along with 10ng, 100ng, or 1000ng of E2 or E2-p53 plasmid. (D) E2 transcriptional activity assay of wild-type E2 and E2-p53. Similar to LCR repression assay, N/Tert-1 cells were transiently transfected with 1 µg pTK6E2-Luciferase reporter plasmid along with increasing amounts of E2 wild-type and E2-p53 plasmids. For (C) and (D), relative luminescence units were calculated by normalizing absolute luminescence readouts to input protein concentration.

bioRxiv preprint doi: https://doi.org/10.1101/2021.11.01.466861; this version posted November 2, 2021. The copyright holder for this preprint (which was not certified by peer review) is the author/funder. All rights reserved. No reuse allowed without permission.

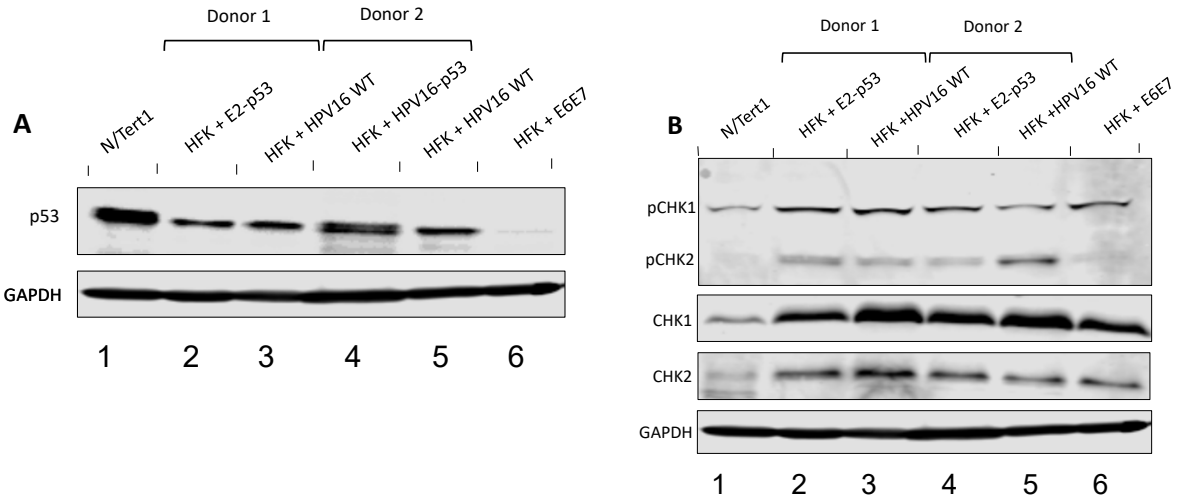

Figure 4. Generation and characterization of HPV16-p53 immortalized human foreskin keratinocytes (HFKs). (A) p53 protein expression in two independent HFK donors immortalized by wild-type HPV16 (Lanes 3 and 5) and HPV-p53 (Lanes 2 and 4). N/Tert-1 and HFK immortalized by E6 and E7 are provided for reference (lanes 1 and 6 respectively). (B) Activation of the ATR and ATM DNA-damage pathways in immortalized HFKs. ATR and ATM activation by HPV16 leads to phosphorylation of Checkpoint kinases 1 and 2 respectively and serve as markers for HPV infection and replication.

bioRxiv preprint doi: https://doi.org/10.1101/2021.11.01.466861; this version posted November 2, 2021. The copyright holder for this preprint (which was not certified by peer review) is the author/funder. All rights reserved. No reuse allowed without permission.

A

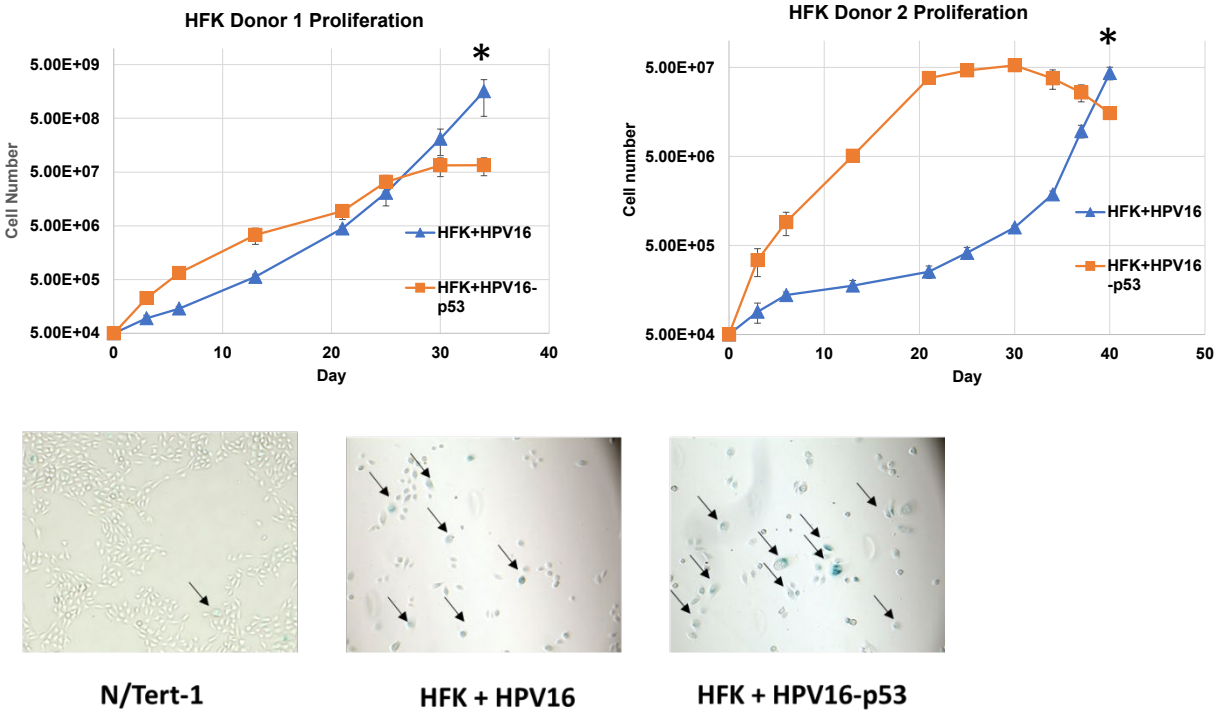

C

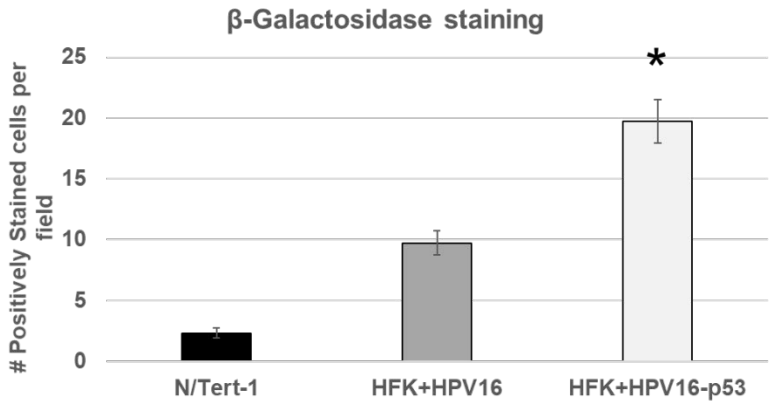

522

523

bioRxiv preprint doi: https://doi.org/10.1101/2021.11.01.466861; this version posted November 2, 2021. The copyright holder for this preprint (which was not certified by peer review) is the author/funder. All rights reserved. No reuse allowed without permission.

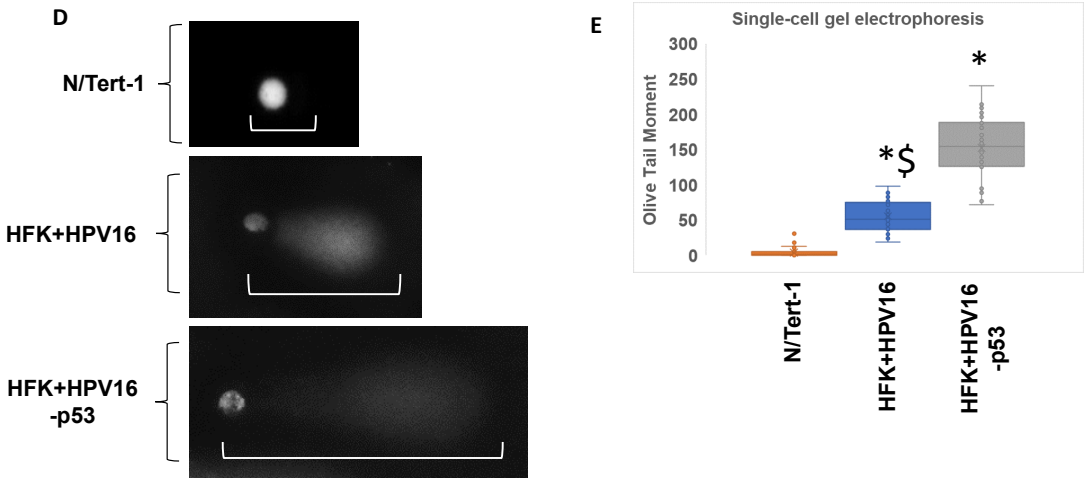

524

525

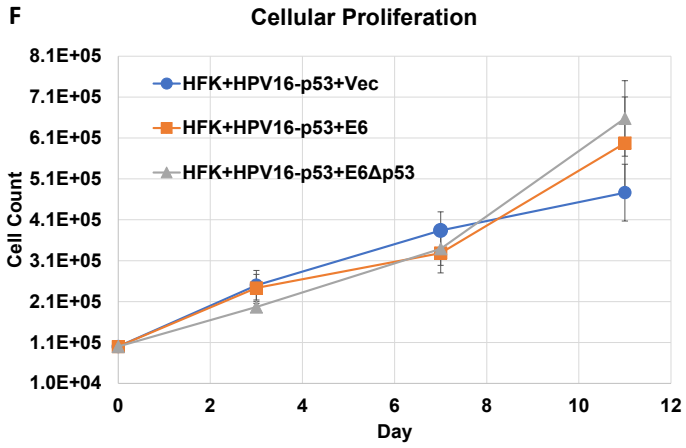

527 **Figure 5. HFKs immortalized by HPV16-p53 exhibit aberrant growth phenotype, elevated**
528 **levels of senescence and increased DNA damage and fragmentation.** (A) Extended growth
529 curve on HFK's immortalized by wild-type HPV16 and HPV16-p53. Cells were grown over a
530 period of 34-40 days depending on HFK donor cell line. In general, donor 1 proliferated quicker
531 than donor 2 regardless of HPV genome status. (B). β-galactosidase staining as a marker of
532 senescence for proliferating HFK+HPV16 and HFK+HPV16-p53 cells compared to N/Tert-1 cells.
533 Images taken at 10X. Five random fields were imaged per replicate per cell line. Representative
534 image presented with positively stained cells marked by arrows. (C) Quantification of β-

bioRxiv preprint doi: https://doi.org/10.1101/2021.11.01.466861; this version posted November 2, 2021. The copyright holder for this preprint (which was not certified by peer review) is the author/funder. All rights reserved. No reuse allowed without permission.

galactosidase staining. Average number of positively stained cells per high power field were calculated by a blinded observer +/- SEM. (D) Single-cell gel electrophoresis (COMET) Assay. Cells were grown in 24-well plate for 24 hours then trypsinized, washed, resuspended in 0.5% low molecular weight agarose, and subjected to single cell gel electrophoresis. DNA was stained with DAPI. Five randomly selected fields were imaged at 20x per replicate per cell line. Representative comets are presented with white bars highlighting comet tails. (E) The olive-tail moments (OTMs) of all non-overlapping comets in each high-power field were were quantified using CaspLab COMET assay software. Average OTM +/- SEM. *$p<0.05$ for HFK+HPV16 vs HFK+HPV16-p53. \$$p<0.05$ for HFK+HPV16 vs N/Tert-1. Bonferoni correction used where applicable. (F). Eleven-day growth curve on HFK+HPV16-p53 stably expressing exogenous E6, E6Δp53 or GFP control.

bioRxiv preprint doi: https://doi.org/10.1101/2021.11.01.466861; this version posted November 2, 2021. The copyright holder for this preprint (which was not certified by peer review) is the author/funder. All rights reserved. No reuse allowed without permission.

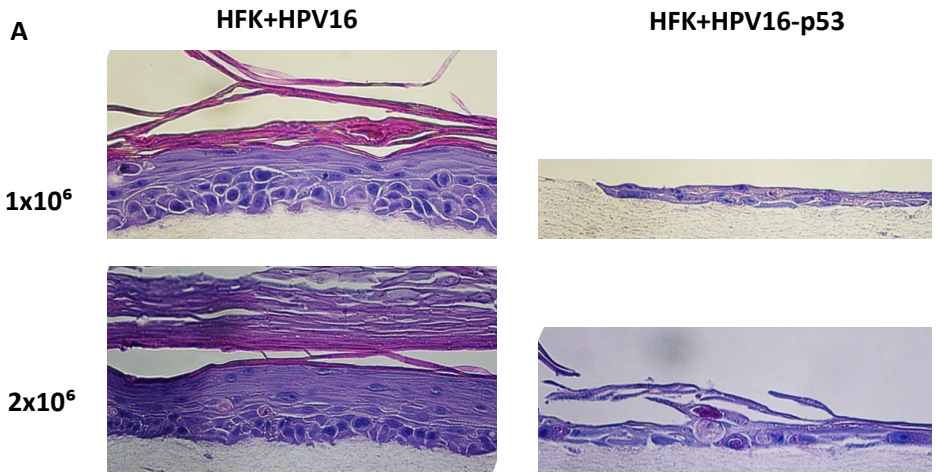

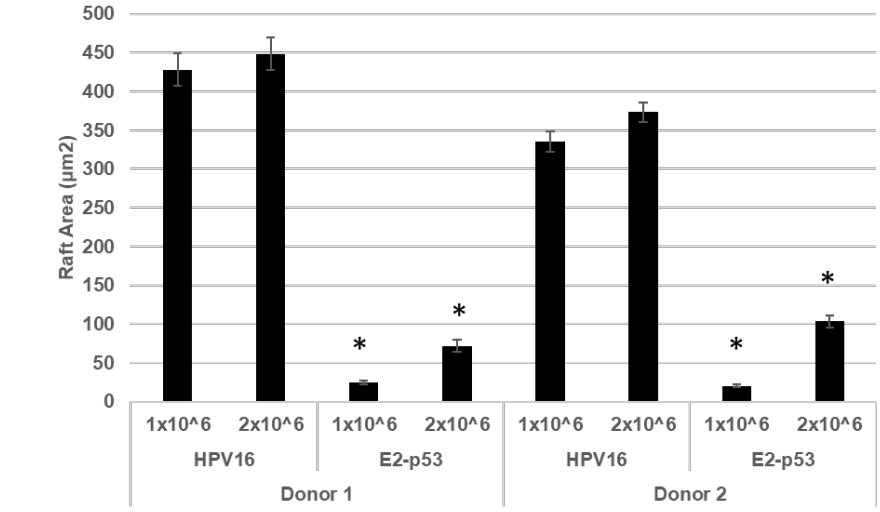

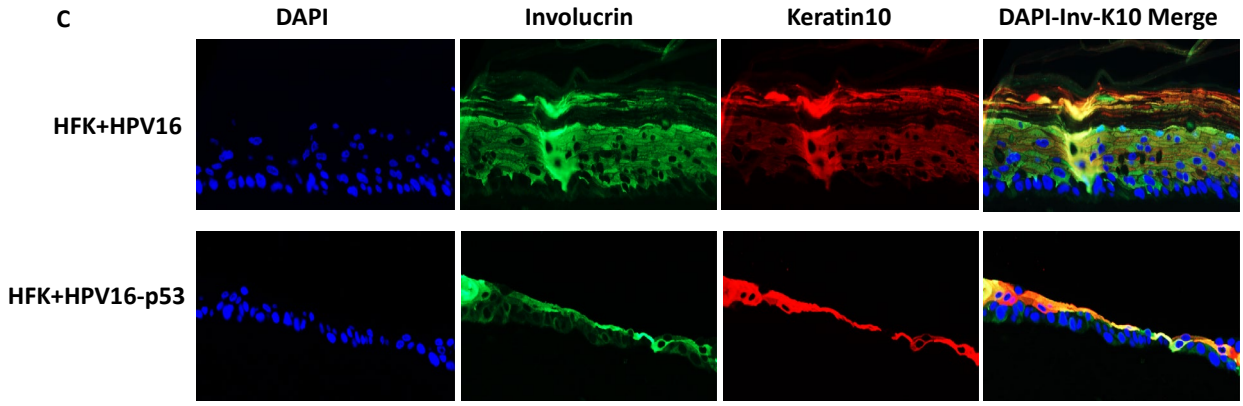

bioRxiv preprint doi: https://doi.org/10.1101/2021.11.01.466861; this version posted November 2, 2021. The copyright holder for this preprint (which was not certified by peer review) is the author/funder. All rights reserved. No reuse allowed without permission.

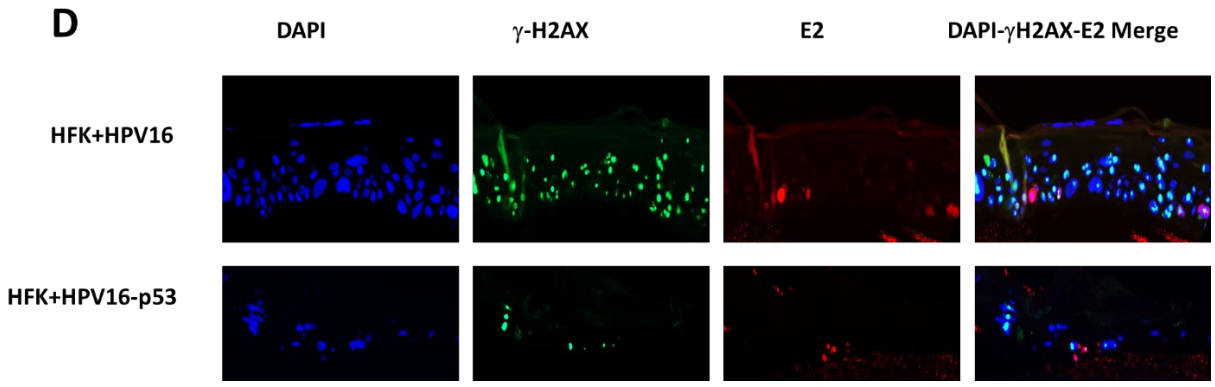

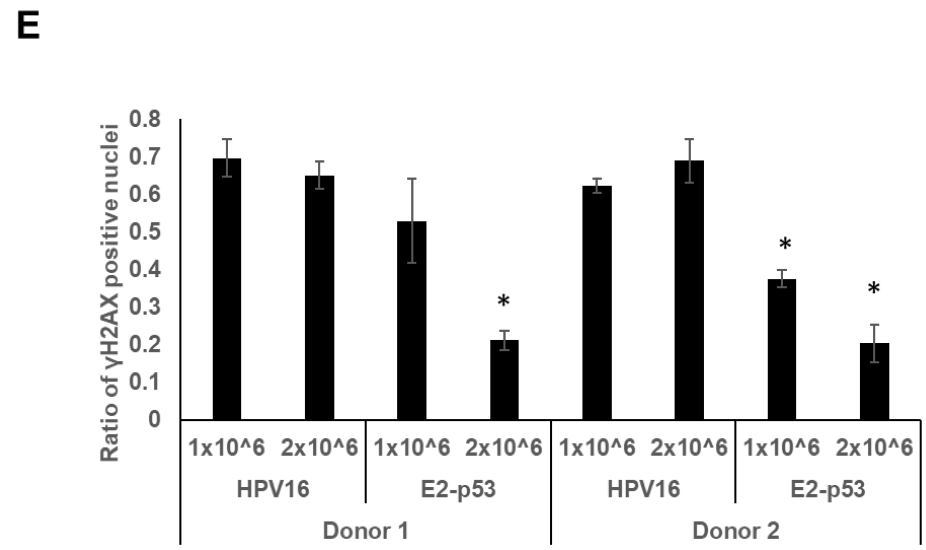

560

561 **Figure 6. Organotypically rafted HFKs immortalized by HPV16-p53 exhibit aberrant life**
562 **cycle with dysregulated differentiation, lower markers of viral replication and overall**
563 **reduced raft proliferation.** (A) Organotypic raft cultures and H&E staining of samples from figure
564 5. HFKs were seeded onto collagen matrices at densities of $1x10^6$ (upper panels) and $2x10^6$
565 (lower panels). (B). The experiment in A was repeated in a second independent HFK donor and
566 average raft areas were calculated for each donor using a Keyence imaging system. (C) HFK
567 rafts stained using indicated antibodies as markers of keratinocyte differentiation. (D) DNA
568 damage and viral replication marker γ-H2AX was stained for in HPV16 and HPV16-p53 HFK rafts.

bioRxiv preprint doi: https://doi.org/10.1101/2021.11.01.466861; this version posted November 2, 2021. The copyright holder for this preprint (which was not certified by peer review) is the author/funder. All rights reserved. No reuse allowed without permission.

(E) γ-H2AX staining was repeated in a second HFK donor and quantified using a Keyence imaging system.

bioRxiv preprint doi: https://doi.org/10.1101/2021.11.01.466861; this version posted November 2, 2021. The copyright holder for this preprint (which was not certified by peer review) is the author/funder. All rights reserved. No reuse allowed without permission.

References:

1. **zur Hausen H.** 2009. Papillomaviruses in the causation of human cancers - a brief historical account. Virology **384:**260-265.
2. **Marur S, D'Souza G, Westra WH, Forastiere AA.** 2010. HPV-associated head and neck cancer: a virus-related cancer epidemic. The Lancet. Oncology **11:**781-789.
3. **Gillison ML, Koch WM, Capone RB, Spafford M, Westra WH, Wu L, Zahurak ML, Daniel RW, Viglione M, Symer DE, Shah KV, Sidransky D.** 2000. Evidence for a causal association between human papillomavirus and a subset of head and neck cancers. Journal of the National Cancer Institute **92:**709-720.
4. **Gillison ML.** 2004. Human papillomavirus-associated head and neck cancer is a distinct epidemiologic, clinical, and molecular entity. Seminars in oncology **31:**744-754.
5. **Chaturvedi AK, Engels EA, Pfeiffer RM, Hernandez BY, Xiao W, Kim E, Jiang B, Goodman MT, Sibug-Saber M, Cozen W, Liu L, Lynch CF, Wentzensen N, Jordan RC, Altekruse S, Anderson WF, Rosenberg PS, Gillison ML.** 2011. Human papillomavirus and rising oropharyngeal cancer incidence in the United States. Journal of clinical oncology : official journal of the American Society of Clinical Oncology **29:**4294-4301.
6. **Thierry F.** 2009. Transcriptional regulation of the papillomavirus oncogenes by cellular and viral transcription factors in cervical carcinoma. Virology **384:**375-379.
7. **Scheffner M, Huibregtse JM, Vierstra RD, Howley PM.** 1993. The HPV-16 E6 and E6-AP complex functions as a ubiquitin-protein ligase in the ubiquitination of p53. Cell **75:**495-505.
8. **Mittal S, Banks L.** 2017. Molecular mechanisms underlying human papillomavirus E6 and E7 oncoprotein-induced cell transformation. Mutation research. Reviews in mutation research **772:**23-35.
9. **Huibregtse JM, Scheffner M, Howley PM.** 1991. A cellular protein mediates association of p53 with the E6 oncoprotein of human papillomavirus types 16 or 18. The EMBO journal **10:**4129-4135.
10. **Thomas M, Pim D, Banks L.** 1999. The role of the E6-p53 interaction in the molecular pathogenesis of HPV. Oncogene **18:**7690-7700.
11. **Hoppe-Seyler K, Bossler F, Braun JA, Herrmann AL, Hoppe-Seyler F.** 2018. The HPV E6/E7 Oncogenes: Key Factors for Viral Carcinogenesis and Therapeutic Targets. Trends in microbiology **26:**158-168.
12. **McBride AA.** 2013. The papillomavirus E2 proteins. Virology **445:**57-79.
13. **Loo YM, Melendy T.** 2004. Recruitment of replication protein A by the papillomavirus E1 protein and modulation by single-stranded DNA. Journal of virology **78:**1605-1615.
14. **Bergvall M, Melendy T, Archambault J.** 2013. The E1 proteins. Virology **445:**35-56.
15. **Stanley MA, Pett MR, Coleman N.** 2007. HPV: from infection to cancer. Biochemical Society transactions **35:**1456-1460.
16. **Stanley MA.** 2012. Epithelial cell responses to infection with human papillomavirus. Clin Microbiol Rev **25:**215-222.
17. **Doorbar J, Quint W, Banks L, Bravo IG, Stoler M, Broker TR, Stanley MA.** 2012. The biology and life-cycle of human papillomaviruses. Vaccine **30 Suppl 5:**F55-70.
18. **Bouvard V, Storey A, Pim D, Banks L.** 1994. Characterization of the human papillomavirus E2 protein: evidence of trans-activation and trans-repression in cervical keratinocytes. The EMBO journal **13:**5451-5459.
19. **McBride AA, Sakakibara N, Stepp WH, Jang MK.** 2012. Hitchhiking on host chromatin: how papillomaviruses persist. Biochimica et biophysica acta **1819:**820-825.

bioRxiv preprint doi: https://doi.org/10.1101/2021.11.01.466861; this version posted November 2, 2021. The copyright holder for this preprint (which was not certified by peer review) is the author/funder. All rights reserved. No reuse allowed without permission.

20. **Fontan CT, Das, D., Bristol, M.L., James, C.D., Wang, X., Lohner, H., Atfi, A., Morgan, I.M.** 2020. Human papillomavirus 16 E2 repression of TWISTI transcrption is a potential mediator of HPV16 cancer outcomes. mSphere **(In press)**.
21. **Evans MR, James CD, Bristol ML.** 2019. Human Papillomavirus 16 E2 Regulates Keratinocyte Gene Expression Relevant to Cancer and the Viral Life Cycle. **93**.
22. **Gauson EJ, Windle B, Donaldson MM, Caffarel MM, Dornan ES, Coleman N, Herzyk P, Henderson SC, Wang X, Morgan IM.** 2014. Regulation of human genome expression and RNA splicing by human papillomavirus 16 E2 protein. Virology **468-470:**10-18.
23. **Gauson EJ, Wang X, Dornan ES, Herzyk P, Bristol M, Morgan IM.** 2016. Failure to interact with Brd4 alters the ability of HPV16 E2 to regulate host genome expression and cellular movement. Virus Res **211:**1-8.
24. **Muller M, Demeret C.** 2012. The HPV E2-Host Protein-Protein Interactions: A Complex Hijacking of the Cellular Network. The open virology journal **6:**173-189.
25. **Yee KS, Vousden KH.** 2005. Complicating the complexity of p53. Carcinogenesis **26:**1317-1322.
26. **Vousden KH, Lane DP.** 2007. p53 in health and disease. Nature Reviews Molecular Cell Biology **8:**275-283.
27. **Romanova LY, Willers H, Blagosklonny MV, Powell SN.** 2004. The interaction of p53 with replication protein A mediates suppression of homologous recombination. Oncogene **23:**9025-9033.
28. **Lane DP.** 1992. Cancer. p53, guardian of the genome. Nature **358:**15-16.
29. **Gatz SA, Wiesmüller L.** 2006. p53 in recombination and repair. Cell Death & Differentiation **13:**1003-1016.
30. **Cheng Q, Chen J.** 2010. Mechanism of p53 stabilization by ATM after DNA damage. Cell Cycle **9:**472-478.
31. **Li S, Hong X, Wei Z, Xie M, Li W, Liu G, Guo H, Yang J, Wei W, Zhang S.** 2019. Ubiquitination of the HPV Oncoprotein E6 Is Critical for E6/E6AP-Mediated p53 Degradation. Front Microbiol **10:**2483-2483.
32. **Vande Pol SB, Klingelhutz AJ.** 2013. Papillomavirus E6 oncoproteins. Virology **445:**115-137.
33. **Martinez-Zapien D, Ruiz FX, Poirson J, Mitschler A, Ramirez J, Forster A, Cousido-Siah A, Masson M, Vande Pol S, Podjarny A, Travé G, Zanier K.** 2016. Structure of the E6/E6AP/p53 complex required for HPV-mediated degradation of p53. Nature **529:**541-545.
34. **Zhou G, Liu Z, Myers JN.** 2016. TP53 Mutations in Head and Neck Squamous Cell Carcinoma and Their Impact on Disease Progression and Treatment Response. Journal of cellular biochemistry **117:**2682-2692.
35. **Poeta ML, Manola J, Goldwasser MA, Forastiere A, Benoit N, Califano JA, Ridge JA, Goodwin J, Kenady D, Saunders J, Westra W, Sidransky D, Koch WM.** 2007. TP53 Mutations and Survival in Squamous-Cell Carcinoma of the Head and Neck. New England Journal of Medicine **357:**2552-2561.
36. **Pim D, Massimi P, Banks L.** 1997. Alternatively spliced HPV-18 E6* protein inhibits E6 mediated degradation of p53 and suppresses transformed cell growth. Oncogene **15:**257-264.
37. **Smotkin D, Wettstein FO.** 1986. Transcription of human papillomavirus type 16 early genes in a cervical cancer and a cancer-derived cell line and identification of the E7 protein. Proc Natl Acad Sci U S A **83:**4680-4684.
38. **Guccione E, Pim D, Banks L.** 2004. HPV-18 E6*I modulates HPV-18 full-length E6 functions in a cell cycle dependent manner. International journal of cancer **110:**928-933.
39. **Schneider-Gädicke A, Schwarz E.** 1986. Different human cervical carcinoma cell lines show similar transcription patterns of human papillomavirus type 18 early genes. The EMBO journal **5:**2285-2292.

bioRxiv preprint doi: https://doi.org/10.1101/2021.11.01.466861; this version posted November 2, 2021. The copyright holder for this preprint (which was not certified by peer review) is the author/funder. All rights reserved. No reuse allowed without permission.

40. **Kösel S, Burggraf S, Engelhardt W, Olgemöller B.** 2007. Increased levels of HPV16 E6*I transcripts in high-grade cervical cytology and histology (CIN II+) detected by rapid real-time RT-PCR amplification. Cytopathology : official journal of the British Society for Clinical Cytology **18:**290-299.
41. **Nulton TJ, Olex AL, Dozmorov M, Morgan IM, Windle B.** 2017. Analysis of The Cancer Genome Atlas sequencing data reveals novel properties of the human papillomavirus 16 genome in head and neck squamous cell carcinoma. Oncotarget **8:**17684-17699.
42. **Webster K, Parish J, Pandya M, Stern PL, Clarke AR, Gaston K.** 2000. The human papillomavirus (HPV) 16 E2 protein induces apoptosis in the absence of other HPV proteins and via a p53-dependent pathway. The Journal of biological chemistry **275:**87-94.
43. **Parish JL, Kowalczyk A, Chen HT, Roeder GE, Sessions R, Buckle M, Gaston K.** 2006. E2 proteins from high- and low-risk human papillomavirus types differ in their ability to bind p53 and induce apoptotic cell death. Journal of virology **80:**4580-4590.
44. **Brown C, Kowalczyk A, Taylor E, Morgan I, Gaston K.** 2008. P53 represses human papillomavirus type 16 DNA replication via the viral E2 protein. Virology journal **5:**5.
45. **Facompre ND, Sahu V, Montone KT, Harmeyer KM, Nakagawa H, Rustgi AK, Weinstein GS, Gimotty PA, Basu D.** 2017. Barriers to generating PDX models of HPV-related head and neck cancer. The Laryngoscope **127:**2777-2783.
46. **Facompre ND, Rajagopalan P, Sahu V, Pearson AT, Montone KT, James CD, Gleber-Netto FO, Weinstein GS, Jalaly J, Lin A, Rustgi AK, Nakagawa H, Califano JA, Pickering CR, White EA, Windle BE, Morgan IM, Cohen RB, Gimotty PA, Basu D.** 2020. Identifying predictors of HPV-related head and neck squamous cell carcinoma progression and survival through patient-derived models.
47. **Suton P, Skelin M, Rakusic Z, Dokuzovic S, Luksic I.** 2019. Cisplatin-based chemoradiotherapy vs. cetuximab-based bioradiotherapy for p16-positive oropharyngeal cancer: an updated meta-analysis including trials RTOG 1016 and De-ESCALaTE. European archives of oto-rhino-laryngology : official journal of the European Federation of Oto-Rhino-Laryngological Societies (EUFOS) : affiliated with the German Society for Oto-Rhino-Laryngology - Head and Neck Surgery **276:**1275-1281.
48. **Gillison ML, Trotti AM, Harris J, Eisbruch A, Harari PM, Adelstein DJ, Jordan RCK, Zhao W, Sturgis EM, Burtness B, Ridge JA, Ringash J, Galvin J, Yao M, Koyfman SA, Blakaj DM, Razaq MA, Colevas AD, Beitler JJ, Jones CU, Dunlap NE, Seaward SA, Spencer S, Galloway TJ, Phan J, Dignam JJ, Le QT.** 2019. Radiotherapy plus cetuximab or cisplatin in human papillomavirus-positive oropharyngeal cancer (NRG Oncology RTOG 1016): a randomised, multicentre, non-inferiority trial. Lancet (London, England) **393:**40-50.
49. **Mehanna H, Robinson M, Hartley A, Kong A, Foran B, Fulton-Lieuw T, Dalby M, Mistry P, Sen M, O'Toole L, Al Booz H, Dyker K, Moleron R, Whitaker S, Brennan S, Cook A, Griffin M, Aynsley E, Rolles M, De Winton E, Chan A, Srinivasan D, Nixon I, Grumett J, Leemans CR, Buter J, Henderson J, Harrington K, McConkey C, Gray A, Dunn J.** 2019. Radiotherapy plus cisplatin or cetuximab in low-risk human papillomavirus-positive oropharyngeal cancer (De-ESCALaTE HPV): an open-label randomised controlled phase 3 trial. Lancet (London, England) **393:**51-60.
50. **Jeremic B, Shibamoto Y, Stanisavljevic B, Milojevic L, Milicic B, Nikolic N.** 1997. Radiation therapy alone or with concurrent low-dose daily either cisplatin or carboplatin in locally advanced unresectable squamous cell carcinoma of the head and neck: a prospective randomized trial. Radiotherapy and oncology : journal of the European Society for Therapeutic Radiology and Oncology **43:**29-37.

bioRxiv preprint doi: https://doi.org/10.1101/2021.11.01.466861; this version posted November 2, 2021. The copyright holder for this preprint (which was not certified by peer review) is the author/funder. All rights reserved. No reuse allowed without permission.

51. **Scarth JA, Patterson MR, Morgan EL, Macdonald A.** 2021. The human papillomavirus oncoproteins: a review of the host pathways targeted on the road to transformation. The Journal of general virology **102**.
52. **White EA, Kramer RE, Tan MJA, Hayes SD, Harper JW, Howley PM.** 2012. Comprehensive analysis of host cellular interactions with human papillomavirus E6 proteins identifies new E6 binding partners and reflects viral diversity. Journal of virology **86:**13174-13186.
53. **Prabhakar AT, James CD, Das D, Otoa R, Day M, Burgner J, Fontan CT, Wang X, Glass SH, Wieland A, Donaldson MM, Bristol ML, Li R.** 2021. CK2 Phosphorylation of Human Papillomavirus 16 E2 on Serine 23 Promotes Interaction with TopBP1 and Is Critical for E2 Interaction with Mitotic Chromatin and the Viral Life Cycle. mBio 12(5) e0116321.
54. **Myers JE, Zwolinska K, Sapp MJ, Scott RS.** 2020. An Exonuclease V-qPCR Assay to Analyze the State of the Human Papillomavirus 16 Genome in Cell Lines and Tissues. Curr Protoc Microbiol **59:**e119.
55. **Myers JE, Guidry JT, Scott ML, Zwolinska K, Raikhy G, Prasai K, Bienkowska-Haba M, Bodily JM, Sapp MJ, Scott RS.** 2019. Detecting episomal or integrated human papillomavirus 16 DNA using an exonuclease V-qPCR-based assay. Virology **537:**149-156.
56. **James CD, Fontan CT, Otoa R, Das D, Prabhakar AT, Wang X, Bristol ML, Morgan IM.** 2020. Human Papillomavirus 16 E6 and E7 Synergistically Repress Innate Immune Gene Transcription. mSphere **5**.
57. **Mehta K, Laimins L.** 2018. Human Papillomaviruses Preferentially Recruit DNA Repair Factors to Viral Genomes for Rapid Repair and Amplification. mBio **9:**e00064-00018.
58. **Gauson EJ, Donaldson MM, Dornan ES, Wang X, Bristol M, Bodily JM, Morgan IM.** 2015. Evidence supporting a role for TopBP1 and Brd4 in the initiation but not continuation of human papillomavirus 16 E1/E2-mediated DNA replication. Journal of virology **89:**4980-4991.
59. **Dahlet T, Argüeso Lleida A, Al Adhami H, Dumas M, Bender A, Ngondo RP, Tanguy M, Vallet J, Auclair G, Bardet AF, Weber M.** 2020. Genome-wide analysis in the mouse embryo reveals the importance of DNA methylation for transcription integrity. Nature communications **11:**3153-3153.
60. **Smith ZD, Meissner A.** 2013. DNA methylation: roles in mammalian development. Nature reviews. Genetics **14:**204-220.
61. **Estève P-O, Chin HG, Pradhan S.** 2005. Human maintenance DNA (cytosine-5)-methyltransferase and p53 modulate expression of p53-repressed promoters. Proc Natl Acad Sci U S A **102:**1000.
62. **Chappell WH, Gautam D, Ok ST, Johnson BA, Anacker DC, Moody CA.** 2015. Homologous Recombination Repair Factors Rad51 and BRCA1 Are Necessary for Productive Replication of Human Papillomavirus 31. Journal of virology **90:**2639-2652.
63. **Anacker DC, Gautam D, Gillespie KA, Chappell WH, Moody CA.** 2014. Productive replication of human papillomavirus 31 requires DNA repair factor Nbs1. Journal of virology **88:**8528-8544.
64. **Gillespie KA, Mehta KP, Laimins LA, Moody CA.** 2012. Human papillomaviruses recruit cellular DNA repair and homologous recombination factors to viral replication centers. Journal of virology **86:**9520-9526.
65. **Bristol ML, James CD, Wang X, Fontan CT, Morgan IM.** 2020. Estrogen Attenuates the Growth of Human Papillomavirus-Positive Epithelial Cells. mSphere **5:**e00049-00020.
66. **James CD, Prabhakar AT, Otoa R, Evans MR, Wang X, Bristol ML, Zhang K, Li R, Morgan IM.** 2019. SAMHD1 Regulates Human Papillomavirus 16-Induced Cell Proliferation and Viral Replication during Differentiation of Keratinocytes. mSphere **4:**e00448-00419.

bioRxiv preprint doi: https://doi.org/10.1101/2021.11.01.466861; this version posted November 2, 2021. The copyright holder for this preprint (which was not certified by peer review) is the author/funder. All rights reserved. No reuse allowed without permission.

763 67. **Evans MR, James CD, Loughran O, Nulton TJ, Wang X, Bristol ML, Windle B, Morgan IM.** 2017.
764 An oral keratinocyte life cycle model identifies novel host genome regulation by human
765 papillomavirus 16 relevant to HPV positive head and neck cancer. Oncotarget **8:**81892-81909.
766 68. **Massimi P, Pim D, Bertoli C, Bouvard V, Banks L.** 1999. Interaction between the HPV-16 E2
767 transcriptional activator and p53. Oncogene **18:**7748-7754.
768 69. **Końca K, Lankoff A, Banasik A, Lisowska H, Kuszewski T, Góźdź S, Koza Z, Wojcik A.** 2003. A
769 cross-platform public domain PC image-analysis program for the comet assay. Mutation
770 research **534:**15-20.
771 70. **James CD, Das D, Morgan EL.** 2020. Werner Syndrome Protein (WRN) Regulates Cell
772 Proliferation and the Human Papillomavirus 16 Life Cycle during Epithelial Differentiation. **5**.
773 71. **Wieland A, Patel MR, Cardenas MA, Eberhardt CS, Hudson WH.** 2020. Defining HPV-specific B
774 cell responses in patients with head and neck cancer.

775